

# Handshakiness: Benchmarking for Human-Robot Hand Interactions

Espen Knoop<sup>1</sup>, Moritz Bächer<sup>1</sup>, Vincent Wall<sup>2</sup>, Raphael Deimel<sup>2</sup>, Oliver Brock<sup>2</sup> and Paul Beardsley<sup>1</sup>

**Abstract**—Handshakes are common greetings, and humans therefore have strong priors of what a handshake should feel like. This makes it challenging to create compelling and realistic human-robot handshakes, necessitating the consideration of human haptic perception in the design of robot hands. At its most basic level, haptic perception is encoded by contact points and contact pressure distributions on the skin.

This motivates our work on measuring the contact area and contact pressure in human handshaking interactions. We present two benchmarking experiments in this regard, measuring the contact locations in human-human/human-robot handshaking and the contact pressure distribution for handshakes with a sensorized palm. We present results from human studies with the benchmarking experiments, providing a baseline for comparison with robot hands as well as presenting new insights into human handshaking. We also show initial work in using these results for the evaluation of robot hands, and progressing towards iterative design of robot hands optimized for social hand interactions.

## I. INTRODUCTION

Recent advances in soft robotics [1, 2] and soft manipulation [3, 4] are laying the foundations for safe, comfortable and friendly physical Human-Robot Interaction (pHRI). Going beyond the commonly considered application of safe shared operating spaces in manufacturing [5], this presents exciting opportunities for robots interacting socially with humans. Applications include robot companions, physical robotic telepresence, prosthetics, toys and entertainment robots. However, the design of safe and natural-feeling physical social human-robot interactions requires focused research and consideration of human haptic perception.

A particularly challenging physical social interaction is that of handshaking (Fig. 1). Handshakes are common interactions throughout the world, and humans therefore have strong priors of what a handshake interaction should feel like. Moreover, the perceived qualities of a handshake contribute to creating first character impressions and forming social bonds. More generally, non-verbal communication has been shown to be five times more important than spoken language with regards to evaluation of friendliness and liking [6]. This motivates our work towards developing soft robotic hands that are capable of realistic handshaking.

From a haptics perspective, physical interactions have a kinesthetic element (joint torques) and a cutaneous element of contact forces on the skin. In this work, we consider the

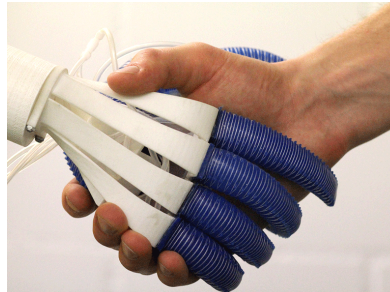


Fig. 1. Humans are sensitive to subtle variations in handshaking, and hence it is challenging to realize a natural robot-human handshake. We benchmark hands to enable natural human-robot interactions.

*cutaneous element* of handshaking interactions, which is affected by factors of the robot hand including hand shape and morphology, hand actuation and the mechanical properties of the skin of the robot hand. This complements existing research on the kinesthetic aspects of an interaction [7, 8].

The fundamental element of cutaneous haptic interaction is contact with the skin, which can be quantified through *contact area*, *contact pressure* and *contact force*. A bottom-up approach to understanding handshaking should therefore measure those quantities, while interfering minimally with the interaction. Although handshaking is a dynamic interaction, we argue that important aspects of the handshake such as hand morphology can be studied without considering variations over time which allows us to design experiments with very high spatial granularity in comparison to existing work.

### A. Contributions

We introduce two benchmarking experiments which measure the non-temporal contact locations and contact pressure in handshaking interactions. Firstly, we measure hand contact locations in a minimally-interfering manner, allowing characterisation of realistic interactions. Secondly, we present an experimental setup for measuring the contact pressure and grasping force in interactions with a hand-like test object. We are able to detect low-pressure contacts down to the limits of human perception.

We perform human handshaking studies with the two experiments, and also include our initial efforts of evaluating robot hands and optimizing hand designs for handshaking interactions. Taken together, the two benchmarks allow us to assess the cutaneous handshaking performance—the ‘handshakiness’—of a robot hand, and provide feedback for informing the robot hand design.

This work has been supported by the European Commission Horizon 2020 Framework Programme, through the Soma project (grant H2020-ICT-645599).

<sup>1</sup>EK, MB and PB are with Disney Research, Stampfenbachstrasse 48, 8006 Zurich, Switzerland [espen.knoop@disneyresearch.com](mailto:espen.knoop@disneyresearch.com)

<sup>2</sup>VW, RD and OB are with Robotics and Biology Laboratory, Technische Universität Berlin, Germany.

## II. RELATED WORK

The approach of studying and mimicking human performance is widely applied in the robotics literature. For robot hands, examples include hand kinematics [9] and hand synergies [4]. Hand kinematics are also considered in evaluating the anthropomorphism of robot hands [10, 11]. As another example of mimicking human-interactions, Fitter and Kuchenbecker [12] systematically study human-robot hand interactions in hand clapping games and teach the games to the robot. Here, we instead look at mimicking the haptic perception element of physical human-robot hand interactions.

Related to aspects of cutaneous haptic perception, Cabibhan et al. [13, 14] present work towards creating robotic skin that feels similar to human skin.

Tsalamlal et al. [15] consider a human-robot handshaking interaction, and evaluate how perceived affective properties of the interaction change as the grasping force, arm stiffness, and the robot’s facial expressions are varied. Pedemonte et al. [16] develop a system targeted at human-robot handshaking interactions, including a robot arm controller, a custom hand and a hand controller. The design of the system is informed by human performance, and the complete system is evaluated in a user study. However, as these studies consider entire robotic systems it is difficult to gain low-level insights into the precise effects of hand properties such as hand morphology.

We argue that for mimicking the perceived haptic qualities of human interactions, the fundamental quantities to study are the contact areas and contact pressure distributions. These quantities have been considered in the ergonomics literature for hand-handle interactions [17, 18], and commercial systems for measuring the contact pressure distribution in a grasp are available such as the Manigraphy System from Novel GmbH and the Grip System from Tekscan, Inc. However, these experiments generally consider values at peak grasping forces on cylindrical test objects, and the results can therefore not readily be transferred to the scenario of handshaking. With regards to the safety of human-robot interactions, recent standardization efforts describe safety thresholds for contact forces and contact pressures at different locations on the human body [19]. However, these thresholds relate to human injury and pain thresholds. For safe and comfortable social human-robot interactions, lower thresholds are required. Contact pressure has also been proposed as an evaluation for soft robotic grippers [20].

Contact forces in human interactions have been measured using sensorized gloves, both for object grasping [21] and for handshaking interactions [22]. Closely related to our work, Tagne et al. [23] study human-human handshaking interactions and measure contact forces along with IMU hand motion data. These systems allow for temporal effects to be captured, but provide sensorization only at particular hand locations and with limited spatial resolution. Our approach is complementary in that it provides high spatial resolution and allows for measurement in any location, but provides no



Fig. 2. Measuring contact area during a handshake. Paint is applied to the hand of one participant, a handshake is performed with a target participant, and the paint-transfer pattern on the target participant’s hand shows the contact area.

temporal information. This high spatial resolution and degree of sensorization is required for capturing small changes in hand morphology and informing design changes.

## III. MEASURING CONTACT AREA

This section describes our method for measuring the contact area during human-human and human-robot hand interactions. Paint is applied to the hand of one participant (we use fingerprint which is non-toxic and easily washable). A handshake is performed with a target participant, and the paint-transfer pattern on the target participant’s hand shows where contact has occurred, as illustrated in Fig. 2. Kamakura et al. [24] use a similar approach, where a human subject grasps an object covered in paint, and the paint-transfer pattern is used to measure grasping prehension patterns. In contrast, we apply the approach to measure hand-to-hand interactions.

Images are taken of the paint-transfer pattern for the palmar and dorsal views of the target participant’s hand. Areas of paint transfer are automatically segmented based on color. The paint-transfer patterns are then warped to a desired 2D hand model. This can be used to register multiple results from a single user, or to register results across users on a generic 2D hand model, enabling direct comparison of contact areas from participants with different hand shapes and sizes.

The above approach can be used to identify the contact area in a human-human handshake and compare it to the contact area for a human-robot interaction. This is useful for robot hand design especially in the optimization of hand morphology and actuation synergies. The approach does not capture temporal information.

### A. Segmentation and Registration of Paint-Transfer Pattern

Images are captured of the palmar and dorsal sides of the hand. The following processing is performed for each of the palmar and dorsal images.

Background subtraction is used to segment the hand from the background, and color segmentation is used to detect areas where paint transfer has occurred, using standard techniques [25]. Next the shape matching algorithm in Belongie et al. [26] is used to match points on the segmented hand silhouette to a generic hand model (in 2D). This provides a mapping to warp the detected paint-transfer pattern to the generic hand model.

TABLE I  
HAND SIZES FOR THE PARTICIPANTS IN THE PAINT TEST STUDY.

Participant	Width (mm)	Circumference (mm)	Length (mm)
1	88	209	170
2	89	210	186
3	89	220	168
4	94	225	185

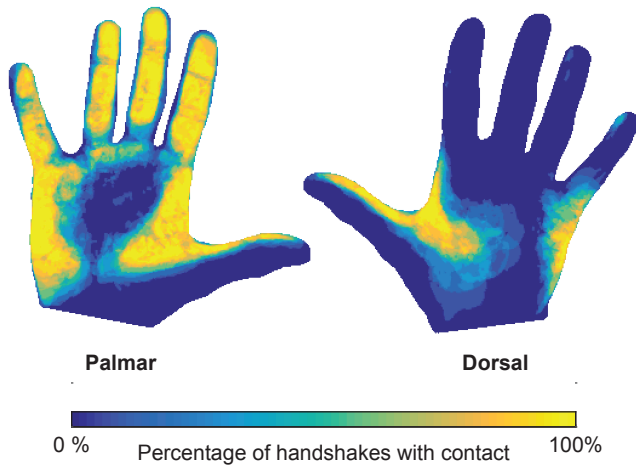


Fig. 3. 2D histogram showing the distribution of contact over all trials of the handshaking interactions. Blue/dark indicates contact in this area in none of the trials, and yellow/light indicates contact in this area in all of the trials.

### B. Study of Human-Human Interactions

1) *Experimental Procedure:* The experiment was carried out with a group of four participants, each performing right-handed handshakes with the other three participants, for a total of 12 distinct pairwise handshakes. Hand sizes of the participants are listed in Tab. I.

2) *Data Analysis:* For the palmar and dorsal faces, the measured paint-transfer/contact areas for the 12 handshakes are mapped onto a generic 2D hand model as described earlier. A histogram is generated in the coordinate frame of the generic hand model, in which each pixel records the number of trials where contact occurred. See Fig. 3—blue/darker areas indicate low contact and yellow/lighter areas indicate higher contact, over all trials of the handshaking.

3) *Results:* Referring to Fig. 3, the palmar side shows little variation in contact area across the set of handshakes. The dorsal side shows somewhat more variation, in both the contact area of the thumb with the back of the hand and also where the fingers wrap around the back of the hand. As there is little variation in hand size across the participants, we attribute this difference to natural variation of the grasping.

4) *Utilizing This Approach:* Fig. 3 is based on human-human handshaking, and provides a benchmark for a human-robot handshake, as described further in Sec. V-A. The most immediate approach is to apply paint to the robot hand and record the contact area on the human hand. However, the converse experiment can also have value. A further insight that can be drawn from Fig. 3 is which parts of the robotic

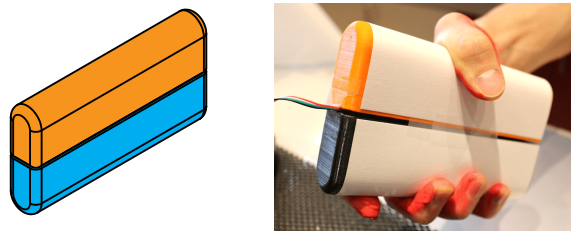


Fig. 4. Sensorized palm for measuring grasping force, contact area, and contact pressure distribution of human and robot hand interactions.

hand are important for handshaking interactions—in areas where contact occurs the shape and surface properties of the robot hand are important whereas in other areas they do not matter. For example, it seems clear that the central part of the palm is not important for handshaking interactions.

### IV. MEASURING CONTACT PRESSURE

The previous section described a method for measuring the contact area of the hand in a real-world handshaking interaction. To provide further insights into the cutaneous haptic element of handshaking, we wish to also measure the *grasping force* and the *contact pressure distribution* over the contact area. As for the contact area measurement, we seek (a) high spatial resolution and (b) sensorization of all hand areas where contact occurs.

It is not feasible to cover a whole human hand with high spatial resolution pressure sensors. We experimented with a Tekscan Grip System, but the sensing area is relatively small and we were unable to identify a sensor placement that would guarantee the measurement of every hand contact in any location. We therefore designed a ‘sensorized palm’—a sensorized object that approximates a human palm<sup>1</sup>, which measures the grasping force, contact area and contact pressure distribution. The whole surface of the sensorized palm is sensorized, so it can be used for evaluating human and robot hands of any morphology and we can guarantee that all contact points are captured.

#### A. Sensorized Palm

The sensorized palm is shown in Fig. 4. It is a flat bar with rounded ends that approximates a human hand, with a developable surface to facilitate sensorization. The device does not capture the geometry of the thumb as this would make the sensorization significantly more challenging. This is a trade-off between device complexity and closeness to the real interaction: a palm with more complex geometry would make the benchmarking experiment far more difficult to reproduce. We note from Fig. 3 that the thumb of the grasping participant wraps around the back of the other’s hand, and we anticipate that this wrap-around will be captured when grasping the sensorized palm.

The body of the sensorized palm is 3D-printed in two halves using an Ultimaker printer, with the surface sanded

<sup>1</sup>We use ‘palm’ to refer to the central part of the hand, palmar and dorsal, apart from the fingers and thumb.



Fig. 5. Calibration samples of Prescale film, showing film color for contact pressures increasing linearly between 0.03 and 0.22 MPa.

to provide a uniform finish. A load cell is mounted between the two halves to provide measurement of grasping force. We made two sensorized palms, with sizes corresponding to the median male and female hand size [27].

The sensorized palm provides three measurements—firstly grasping force using the load cell. Secondly, we measure the contact area on the sensorized palm using the paint test described in the previous section—paint is applied to the human hand, and we record the paint pattern transferred to a sheet of paper wrapped around the sensorized palm. Thirdly, the measurement of contact pressure is discussed below.

### B. Contact Pressure Sensing

Contact pressure is measured by wrapping the surface of the sensorized palm with a pressure-sensitive film (Prescale, Fujifilm Corp.), which changes color with applied pressure. The film is single use and has high spatial resolution ( $\sim 0.1$  mm). The dynamic range of the film is limited, and different sensitivity grades are available depending on the required pressure sensing range. The ‘4LW’ grade (lowest pressure, rated as 0.05–0.2 MPa) is well suited for pressures arising in common human hand interactions, while the ‘3LW’ grade (0.2–0.6 MPa) is suited for maximal pressures exerted by human hands. We find that with appropriate calibration the range of the ‘4LW’ grade can be extended to 0.03–0.25 MPa.

After each experiment, the film is scanned and we automatically estimate the contact pressure from the film color value. We apply a low-pass smoothing filter to the image to remove film granularity, and then estimate the contact pressure from the green channel intensity. A separate calibration experiment was performed where known pressures were applied to the film, the film color was recorded, and the relationship between green channel intensity and contact pressure was observed. We found that a quadratic function describes the relationship well. Fig. 5 shows an example set of calibration samples.

The main advantage of using the Prescale film is that it provides very high spatial resolution allowing for fine-grained evaluation of handshaking grasps. The film can be cut to shape using a laser cutter, which offers the potential to sensorize different object shapes with developable surfaces. The cost is also considerably lower than for suitable electronic sensing systems. The single-use nature of the film means that repeated experiments are time-consuming, but this was an acceptable trade-off for our work.

The Prescale film has a minimum activation pressure, and our observation is that the human sense of touch detects contact pressures significantly lower than this threshold. By combining the Prescale film with the paint test, we are able to also identify areas of low-pressure contact which could be important for haptic perception.

TABLE II  
MEAN AND STANDARD DEVIATION OF PARTICIPANT HAND SIZES, CONTACT PRESSURE STUDY.

	$\mu$	$\sigma$
Width (mm)	90.3	3.0
Circumference (mm)	211.3	8.2
Length (mm)	180.1	8.7

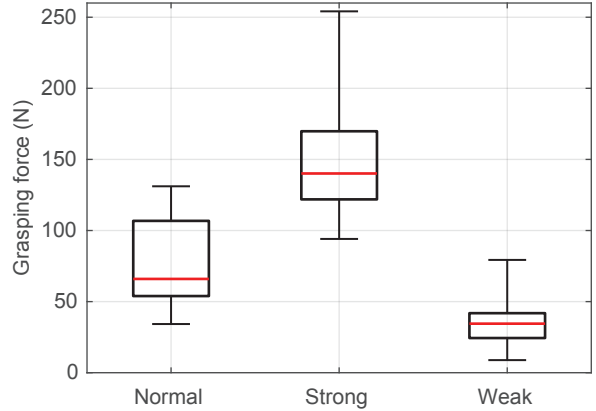


Fig. 6. Boxplot showing handshake grasping force for ‘normal’, ‘strong’ and ‘weak’ handshakes.

### C. Human Study, Handshake Grasping Force

Leading up to the study of contact pressure distributions, we first consider the grasping forces of handshakes. Eight participants were asked to perform different handshakes with the sensorized palm, to give an indication of the magnitude and spread of grasping forces. The participant hand sizes are summarized in Tab. II.

We asked participants to perform ‘normal’, ‘weak’ and ‘strong’ handshakes with each of the sensorized palms (male and female size), while the grasping force was recorded. Each handshake strength was repeated 3 times for the male and female handle sizes. We take the grasp force as the peak force measured by the load cell. The resulting grasping forces are presented in a boxplot in Fig. 6, where the whiskers show the maximum and minimum values. We observe no difference for grasping strength results with the male- and female-sized sensorized palm so these results have been combined.

It can be seen that there is some variation across the participants. The median value for a ‘normal’ handshake is 66 N, with 25th and 75th percentiles respectively being 54 and 107 N. There is separation between the interquartile ranges for the three strengths, but overlap in the extremal values.

### D. Human Study, Contact Pressure Distributions

Next, we performed a study to measure the contact pressure distributions in human handshakes. This forms a baseline which can be used to quantitatively evaluate the handshaking performance of robot hands. The participants

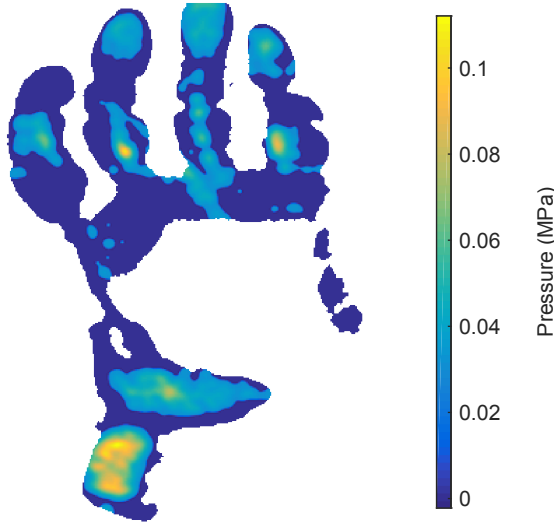


Fig. 7. Contact pressure and contact area for a single trial. The grasping force in this trial was 46.9 N.

were the same as for the handshake grasping force experiment.

Participants were asked to perform a single ‘normal’ handshake with the sensorized palm. We recorded the contact area, contact pressure and grasping force as described above. The contact area and contact pressure measurements were combined to show contact areas with contact pressure below the range of the Prescale film.

As an illustrative example, Fig. 7 shows the contact pressure distribution for a single trial. It can be seen that the distribution of contact area is similar to that seen in human-human handshaking (Fig. 3): the thumb and fingers wrap around the sides of the handle and contact is made around the edges of the palm.

These results provide the basis for a discussion about the quantitative properties of contacts in human handshaking interactions.

1) *Force and Contact Area:* We hypothesize a possible positive correlation between grasping force  $F$  and contact area  $A$ . However, this trend is not observed in our data: we find a correlation coefficient between  $F$  and  $A$  of  $R^2 = 0.019$ . Contact area has a mean value of  $5500 \text{ mm}^2$ , with a standard deviation of  $700 \text{ mm}^2$ .

2) *Peak Contact Pressure and Force:* The peak contact pressure  $P_{max}$  is an important metric for the evaluation of robot handshake quality: we wish to avoid high localized contact pressure which may cause discomfort or pain, as might occur with a rigid robot hand. We expect a positive correlation between  $F$  and  $P_{max}$ . Fig. 8 shows a plot of the grasping force against the peak contact pressure for our dataset. A positive correlation is observed ( $R^2 = 0.41$ ). Note that in 4 trials the pressure-sensitive film saturated at its maximum value—these points are shown in pale grey and were excluded when computing the correlation coefficient.

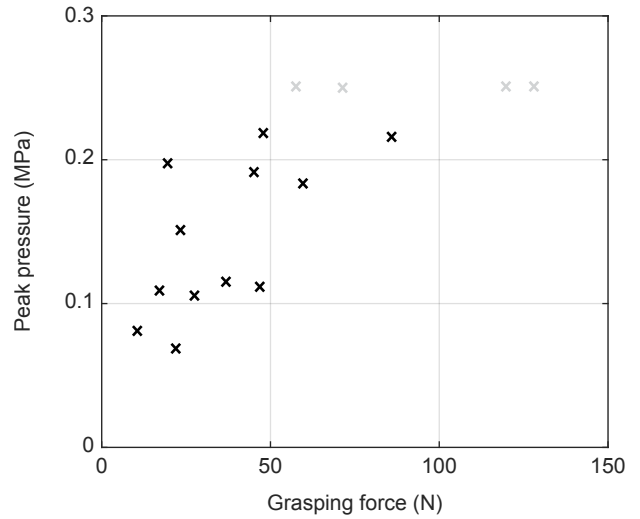


Fig. 8. Peak contact pressure  $P_{max}$  against grasping force  $F$ : Pale grey points indicate that the pressure-sensitive film was saturated.

3) *Peak Contact Pressure and Sharpness of Peaks:* To evaluate the sharpness of the high-pressure peaks in the contact pressure distribution, we define the quantity  $\Sigma P$  to be the sum of contact pressure over the contact area. If the contact area was unwrapped to a flat surface, this would equate to the resultant force on the surface. The ratio of  $P_{max}$  and  $\Sigma P$  is then a measure of the narrowness of the contact pressure distribution: a contact pressure with localized high-pressure peaks will produce a high value while a uniform contact pressure will produce a minimal value. Note that it is more informative to use  $\Sigma P$  than to use  $F$ , as  $F$  only measures the force in the direction of the principal axis of the sensorized palm. Fig. 9 shows a plot of  $P_{max}$  against  $\Sigma P$ . Again, pale grey points indicate saturation of the pressure-sensitive film. A positive correlation is observed ( $R^2 = 0.43$ , excluding saturated points).

4) *Handshake Adaptation:* In the real world, we would expect the handshake strength to be adapted to the handshaking partner (e.g., a handshake with a child would be softer than a handshake with a bodybuilder). Our results indicate that  $P_{max}$  and  $\Sigma P$  are correlated with  $F$ , and it is possible that these trends hold across the range of handshake and strengths. This would then provide another level of granularity for robot hand evaluation. However, further experiments are required to explore this in more detail. As a first test, we performed a single trial of a human grasping the handle at peak force (using Prescale 3LW). We measured values of  $F = 509 \text{ N}$ ,  $P_{max} = 0.71 \text{ MPa}$  and  $\Sigma P = 335 \text{ N}$ . Comparing this to the handshaking results in Figs. 8 and 9, it would seem that the relationships become nonlinear at high grasping forces.

## V. INITIAL EVALUATION OF SOFT ROBOT HANDS

This paper has introduced benchmarking metrics for human-robot handshaking, and presented results from human studies. This section presents our efforts towards the

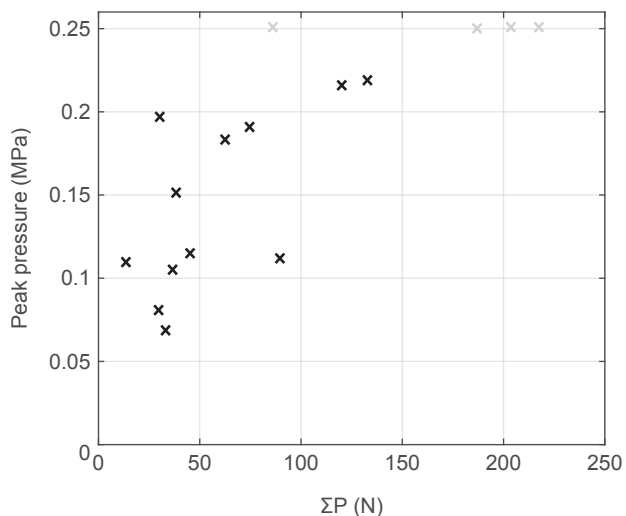


Fig. 9. Plot showing the peak contact pressure  $P_{max}$  against the summed contact pressure  $\Sigma P$ . Pale grey points indicate that the pressure-sensitive film was saturated.

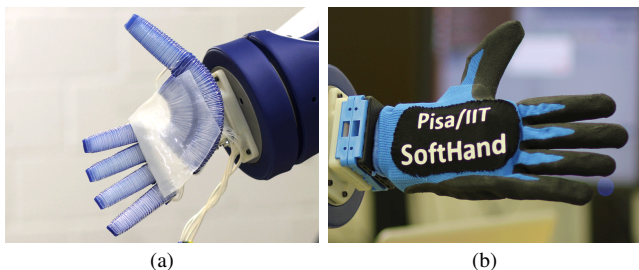


Fig. 10. Robot hands studied here: (a) RBO Hand 2 [3]; (b) Pisa/IIT SoftHand [4].

evaluation of soft robot hands (Fig. 10) using these metrics, and using this to inform and improve robot hand design.

#### A. Contact area metric

We performed the contact area test described in Sec. III on the RBO Hand 2 [3], following the experimental procedure as described before. We wish to optimize for human haptic perception, so paint was applied to the robot hand and the resulting pattern on the human hand was registered. Fig. 11 shows the registered contact area for the interactions with the RBO Hand 2, overlaid on the human-human results from Fig. 3.

Comparing the results from the RBO Hand 2 with the results from human-human handshaking, it can be seen that much less contact is made with the palm of the human hand. Looking at the RBO Hand 2 (Fig. 10(a)), this result can be explained from the lack of defined sides of the palm. As a first step towards improving this result, we designed the RBO Hand 2P (Fig. 12) which features a rigid 3D-printed palm in the shape of a human palm. In a user study, 15 participants rated the RBO Hand 2P as having an improved handshake quality over the RBO Hand 2, with no difference in the rated perceived safety.

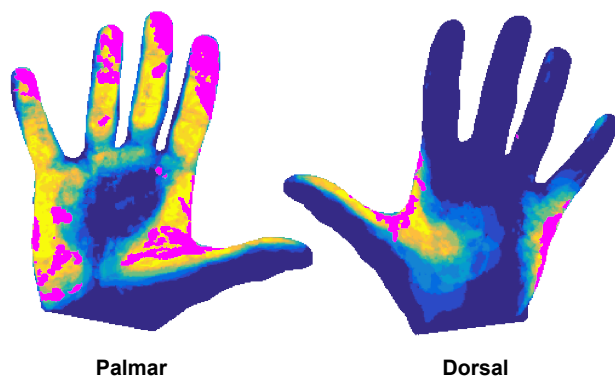


Fig. 11. Contact area from handshaking with RBO Hand 2 (pink), overlaid on the human-human results from Fig. 3.

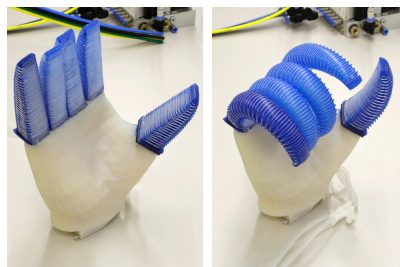


Fig. 12. The RBO Hand 2P, featuring a rigid palm in the shape of a human palm.

#### B. Contact Pressure Distributions

We measured the contact pressure distribution and grasping force of the Pisa/IIT SoftHand [4], as described in Sec. IV. Due to high peak pressures, this required us to use the ‘3LW’ grade of Prescale film.

We measured a grasping force  $F$  of 50 N and a peak contact pressure  $P_{max}$  of 0.51 MPa. Compared to the maximal-strength human grasp, this is a similar peak pressure value at a grasping force which is an order of magnitude smaller. In informal experiments, we have found that the Pisa/IIT SoftHand is capable of performing uncomfortable and painful handshakes at a grasping force of 50 N (which would be classed at the lower end of ‘normal’ handshake, c.f. Fig. 6). We have discussed this previously [28], and in collaboration with the University of Pisa, we are currently working towards improving the performance of the SoftHand in this regard.

#### C. Exploring the Design Space of Soft Robot Fingers

As a more specific example of how the benchmarking metrics could be used in the design of robot hands, we explored the design space of PneuFlex pneumatic actuators [3] as used in the RBO Hand 2. We evaluated the ability of different fingers to wrap around the edge of the sensorized palm, as would be required in a handshaking interaction.

The PneuFlex is a pneumatic continuum actuator, where the cross-section along the length of the finger determines the compliance and actuation behavior. A detailed description of the geometric relationships is presented by Deimel and

TABLE III  
PARAMETERS OF PNEUFLEX DESIGN SPACE SAMPLES.

Finger Version	Stiffness Profile	Actuation Ratio Profile	Nominal Stiffness	Finger Length
P10	linear decrease	constant	100%	90 mm
P11	linear decrease	constant	220%	90 mm
P13	quadratic decrease	constant	220%	110 mm
P15	linear decrease	linear increase	80%	110 mm
P16	linear decrease	linear decrease	80%	110 mm
P17	base: constant, tip: quadratic	constant	200%	130 mm

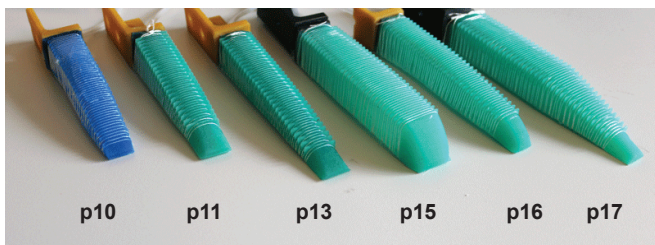


Fig. 13. The evaluated PneuFlex actuator designs, as described in Tab. III. The different finger shapes are a result of the changes in cross-sections.

Brock [3]. We can create actuators with different functionality by varying their design parameters. To test the benchmarking metric with samples from the design space, we built six actuator prototypes (Tab. III, Fig. 13) that vary the following four properties:

- The **stiffness profile** determines the relative bending stiffness along the actuator. A finger with a linearly decreasing profile is stiffest at the base and softer at the fingertip.
- The **actuation ratio profile** specifies the pressure-to-curvature relationship along the actuator. It can be constant, linearly increasing, or linearly decreasing from base to tip.
- The **nominal stiffness** is given in percent of the original PneuFlex design’s stiffness. A high value indicates higher inherent stiffness.
- The **finger length** is measured between base and tip. As the PneuFlex is a continuum actuator, a different length allows to align the finger base differently, creating different contact distributions.

We evaluated each finger design using the sensorized palm introduced in Sec. IV-A. The surface of the male-sized device was covered with the more sensitive ‘4LW’ grade film. The base of the actuator was attached to the side of the palm, so that the finger wrapped around it when inflated. Each actuator was then manually inflated to its maximum pressure, and the resulting contact pressure distribution was measured.

The results shown in Fig. 14 represent data points in the design space spanned by the prototypes. While not spanning the space, this hints at commonalities within the design space and properties that can be varied. When comparing the pressure distributions of the prototypes, we can make a few notable observations. The prototypes P10 and P16 make contact along a longer line than, e.g., the stiffer P11 finger.

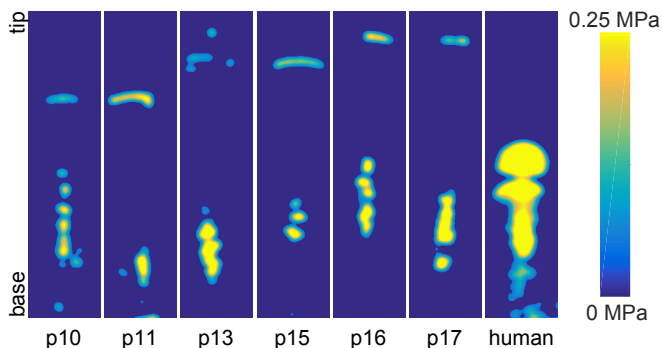


Fig. 14. Pressure distribution on the sensorized palm of the design space samples and a human finger. The length of the human finger is 90 mm.

When comparing to the human finger this seems desirable.

The PneuFlex actuators create contact areas that are smaller than for the human finger. Fingers P13 and P17 show the best performance in this regard. All prototypes also have a pressure point at the fingertip, which is most pronounced in P11 and P16. This would likely cause discomfort in a human interaction.

Our results show that the parameters we explored here have some influence on the contact area and pressure. However, the pressure distribution from the PneuFlex fingers is still significantly different to that of a human finger. It seems that the parameter space studied here is not sufficient to reproduce the human distribution and other design changes are also required. One promising approach we are exploring is to mimic the soft finger pulp of a human finger in the PneuFlex actuators using elastomers and gels.

It can be seen that the benchmarking approach taken here allows us to focus on specific aspects of robot hand designs before creating full hand prototypes.

## VI. DISCUSSION

In the real world, handshakes are different across the population and individuals may also adapt their handshake depending on who they interact with. Sophisticated robotic systems should also exhibit such adaptation. However, we observe that many factors of handshaking show little variation across the human population and far greater variation for current robotic hands (e.g. hand morphology and skin properties). This is exemplified by Fig. 11. At this stage of research, it is therefore more meaningful to average across sets of human handshakes to capture properties that are consistent across human handshakes. In our experiment, we did not give participants specific instructions, so our data should capture natural variation within and between participants. Once a certain level of performance in robot hands is obtained with respect to the benchmarks presented here, attention could be directed at producing more subtle variations.

The metrics introduced in this paper do not consider variations over time, which are clearly important for creating realistic dynamic interactions. However, many hand properties such as hand morphology and local surface properties are

constant and it is therefore more appropriate to study them in a non-temporal manner. For initial hand optimization, such properties should be considered. Our approach could be used for initial coarse-level hand optimization, before considering temporal elements, and also in later optimization stages for tuning local surface contacts. This justifies our approach taken here of performing non-temporal benchmarking experiments. Again, we point to the literature for studies of temporal variation at lower spatial resolution [22, 23].

Our benchmarking tests are useful for informing hand design at different levels of granularity. This includes design parameters such as hand morphology, as demonstrated with the RBO Hand 2P, and actuation synergies, which will lead to large global changes in the contact area and pressure distribution. The local properties of the hand contact will be affected by hand properties including actuation synergies, finger actuator design and hand surface properties.

Although the focus of this paper has been on handshakes, other social physical human-robot interactions also require consideration of the perceived haptic sensation and could benefit from implementing similar methods. This includes other greeting interactions such as hugging, and healthcare applications where robots could be supporting or lifting patients.

## VII. CONCLUSION

We have presented two new benchmarking experiments for characterizing the cutaneous haptic element of handshaking, allowing for the ‘handshakiness’ of robot hands to be evaluated. We have used these benchmarks to measure properties of human handshaking, specifically the hand contact area and contact pressure distribution as well as the grasping force. In addition to providing a baseline for comparison with robot hands, this also provides new insights into human handshaking. We have presented sample results of using the benchmarks for evaluation of robot hands, which paves the way towards optimization of hand designs for handshaking using benchmarking metrics.

## ACKNOWLEDGMENT

We thank Antonio Bicchi, Gaspare Santaera and Giorgio Grioli at Centro di Ricerca ‘E. Piaggio’, University of Pisa, for providing us with a Pisa/IIT SoftHand.

## REFERENCES

- [1] A. Albu-Schaffer, O. Eiberger, M. Grebenstein, S. Haddadin, C. Ott, T. Wimbock, S. Wolf, and G. Hirzinger, ‘‘Soft robotics,’’ *IEEE Robotics & Automation Magazine*, vol. 15, no. 3, 2008.
- [2] D. Rus and M. T. Tolley, ‘‘Design, fabrication and control of soft robots,’’ *Nature*, vol. 521, no. 7553, pp. 467–475, 2015.
- [3] R. Deimel and O. Brock, ‘‘A novel type of compliant and underactuated robotic hand for dexterous grasping,’’ *Int. J. Robotics Research*, vol. 35, no. 1-3, pp. 161–185, 2016.
- [4] M. G. Catalano, G. Grioli, A. Serio, E. Farnioli, C. Piazza, and A. Bicchi, ‘‘Adaptive synergies for a humanoid robot hand,’’ in *Humanoid Robots (Humanoids), 12th IEEE-RAS Int. Conf.* IEEE, 2012, pp. 7–14.
- [5] S. Haddadin and E. Croft, *Physical Human–Robot Interaction*. Springer International Publishing, 2016, pp. 1835–1874.
- [6] M. Argyle, *Bodily communication*. Routledge, 2013.
- [7] E. Giannopoulos, Z. Wang, A. Peer, M. Buss, and M. Slater, ‘‘Comparison of people’s responses to real and virtual handshakes within a virtual environment,’’ *Brain Research Bulletin*, vol. 85, no. 5, pp. 276–282, 2011.
- [8] T. Bhattacharjee and G. Niemeyer, ‘‘Antagonistic muscle based robot control for physical interactions,’’ in *Robotics and Automation (ICRA), Proc. IEEE Int. Conf.* IEEE, 2015, pp. 298–303.
- [9] M. Grebenstein, M. Chalon, G. Hirzinger, and R. Siegart, ‘‘A method for hand kinematics designers 7 billion perfect hands,’’ in *Proc. Int. Conf. Applied Bionics and Biomechanics (ICABB)*, 2010.
- [10] M. V. Liarokapis, P. K. Artemiadis, and K. J. Kyriakopoulos, ‘‘Quantifying anthropomorphism of robot hands,’’ in *Robotics and Automation (ICRA), Proc. IEEE Int. Conf.* IEEE, 2013, pp. 2041–2046.
- [11] B. Leon, C. Rubert, J. Sancho-Bru, and A. Morales, ‘‘Evaluation of prosthetic hands prehension using grasp quality measures,’’ in *Intelligent Robots and Systems (IROS), IEEE/RSJ Int. Conf.* IEEE, 2013, pp. 3501–3506.
- [12] N. T. Fitter and K. J. Kuchenbecker, ‘‘Using IMU data to demonstrate hand-clapping games to a robot,’’ in *Intelligent Robots and Systems (IROS), IEEE/RSJ Int. Conf.* IEEE, 2016, pp. 851–856.
- [13] J. J. Cabibihan, R. Pradipta, Y. Z. Chew, and S. S. Ge, ‘‘Towards humanlike social touch for prosthetics and sociable robotics: Handshake experiments and finger phalange indentations,’’ *Lecture Notes in Computer Science*, vol. 5744, pp. 73–79, 2009.
- [14] J. J. Cabibihan, D. Joshi, Y. M. Srinivasa, M. A. Chan, and A. Murganathanam, ‘‘Illusory sense of human touch from a warm and soft artificial hand,’’ *Trans. Neural Systems and Rehabilitation Engineering*, vol. 23, no. 3, pp. 517–527, 2015.
- [15] M. Y. Tsalamlal, J.-C. Martin, M. Ammi, A. Tapus, and M.-A. Amorim, ‘‘Affective handshake with a humanoid robot: How do participants perceive and combine its facial and haptic expressions?’’ *Proc. 6th Conf Affective Computing and Intelligent Interaction*, pp. 334–340, 2015.
- [16] N. Pedemonte, T. Lalibert e, and C. Gosselin, ‘‘Design, control, and experimental validation of a handshaking reactive robotic interface,’’ *J. Mechanisms and Robotics*, vol. 8, no. 1, p. 011020, 2015.
- [17] Y. Aldien, D. Welcome, S. Rakheja, R. Dong, and P.-E. Boileau, ‘‘Contact pressure distribution at hand-handle interface: role of hand forces and handle size,’’ *Int. J. Industrial Ergonomics*, vol. 35, no. 3, pp. 267 – 286, 2005.
- [18] J. W. Nicholas, R. J. Corvese, C. Woolley, and T. J. Armstrong, ‘‘Quantification of hand grasp force using a pressure mapping system,’’ *Work*, vol. 41, pp. 605–612, 2012.
- [19] ISO/TS 15066:2016, *Robots and robotic devices - Collaborative robots*. International Organization for Standardization, Geneva, Switzerland, 2016.
- [20] K. C. Galloway, K. P. Becker, B. Phillips, J. Kirby, S. Licht, D. Tchernov, R. J. Wood, and D. F. Gruber, ‘‘Soft robotic grippers for biological sampling on deep reefs,’’ *Soft Robotics*, vol. 3, no. 1, pp. 23–33, 2016.
- [21] S. Shimizu, M. Shimojo, S. Sato, Y. Seki, A. Takahashi, Y. Inukai, and M. Yoshioka, ‘‘The relationship between human grip types and force distribution pattern in grasping,’’ in *Advanced Robotics (ICAR), Proc. 8th Int. Conf.* IEEE, 1997, pp. 299–304.
- [22] Z. Wang, J. Hoellampf, and M. Buss, ‘‘Design and performance of a haptic data acquisition glove,’’ *Proc. 10th Ann. Int. Workshop Presence.*, pp. 349–357, 2007.
- [23] G. Tagne, P. H enaff, and N. Gregori, ‘‘Measurement and analysis of physical parameters of the handshake between two persons according to simple social contexts,’’ in *Intelligent Robots and Systems (IROS), IEEE/RSJ Int. Conf.* IEEE, 2016, pp. 674–679.
- [24] N. Kamakura, M. Matsuo, H. Ishii, F. Mitsuboshi, and Y. Miura, ‘‘Patterns of static prehension in normal hands,’’ *American Journal of Occupational Therapy*, vol. 34, no. 7, pp. 437–445, 1980.
- [25] G. Bradski and A. Kaehler, *Learning OpenCV: Computer vision with the OpenCV library*. O’Reilly Media, Inc., 2008.
- [26] S. Belongie, J. Malik, and J. Puzicha, ‘‘Shape matching and object recognition using shape contexts,’’ *IEEE Trans. Pattern Analysis and Machine Intelligence*, vol. 24, no. 4, pp. 509–522, 2002.
- [27] A. Poston, ‘‘Human engineering design data digest,’’ *Washington, DC: Department of Defense Human Factors Engineering Technical Advisory Group*, 2000.
- [28] E. Knoop, M. B acher, and P. Beardsley, ‘‘Contact pressure distribution as an evaluation metric for human-robot hand interactions,’’ in *HRI 2017 Workshop: Towards Reproducible HRI Experiments: Scientific Endeavors, Benchmarking and Standardization*, 2017.